A Load and Time-Dependent Hazardous Materials Distribution Problem in Urban Areas

Eleni Karouti*[a], Konstantinos N. Androutsopoulos[a], Konstantinos G. Zografos[b]

[a] Department of Management Science and Technology, School of Business, Athens University of Economics and Business, 76 Patission str., 104 34, Athens, Greece; [b] Lancaster University Management School, Department of Management Science, Centre for Transport and Logistics (CENTRAL), Lancaster, LA1 4YX, United Kingdom

*email: elenikarouti@gmail.com

Abstract

The objective of this paper is to model and solve the hazardous materials distribution problem in which a set of orders is serviced by a heterogeneous fleet of tank trucks. The objective of the problem is to determine the delivery routes of the trucks so that all the orders are serviced at the minimum traversed distance and transportation risk. A new transportation risk measure is proposed, which takes into account: i) the population exposed within a load-dependent, impacted area around the truck, and ii) the travel speed of the vehicle. Moreover, the proposed problem incorporates the effect of the scheduling of the loading operations performed at the depot into the routing problem. The proposed problem is modeled by a bi-objective vehicle routing and scheduling problem, which apart from determining delivery routes, deals simultaneously with the scheduling of the loading operations at the depot. To address the bi-objective routing and scheduling problem, we have developed an NSGA-II algorithm, known as a non-dominated sorting genetic algorithm, with various novel features. The results of the performed experiments indicate that the proposed risk measure substantially reduces the duration that the population stays under the risk of a HazMat shipment.

Keywords: Vehicle Routing; HazMat Transportation; NSGA-II; Scheduling; Loading Activities

1. Introduction

The transportation of hazardous materials (HazMat) is an essential aspect of modern society, but it also poses a significant risk to public safety and the environment. A HazMat accident may result in environmental and economic damages and put at risk human lives residing within an extended area around the accident location. An effective proactive way of mitigating the risk associated with HazMat shipments is to incorporate safety criteria and constraints in planning transportation activities. HazMat transportation is performed by many different means of transport, however we focus our study on road transportation. This type of transportation activity accounts for 83 % of the total HazMat quantity transported in the U.S. (U.S. DOT, 2017) while road incidents involving HazMat have a share of 93% out of all HazMat-related incidents in the U.S. (U.S. DOT, 2022).

The work presented in this paper is on the Hazardous Materials Vehicle Routing Problem (HMVRP) which aims to determine distribution routes for delivering a set of HazMat orders by a given fleet of trucks at minimum transportation cost and risk. The HMVRP entails the distribution of a diverse set of perilous substances across several sectors, encompassing chemicals, healthcare, and manufacturing, like collecting explosive wastes for recycling (Zhao & Zhu, 2016) or the distribution of liquefied petroleum gas (LPG) (Panicker & Mohammed, 2018).

The field of Hazardous Materials routing problems has witnessed extensive research efforts, reflecting its critical importance in ensuring the safe and efficient transportation of hazardous materials. A considerable amount of academic research has been devoted to finding optimal and safe pathways for transporting hazardous materials through a roadway network (Zero et al., 2019; Bronfman et al., 2015; Androutsopoulos & Zografos, 2010; Carotenuto et al., 2007; Erkut and Alp, 2007; Frank et al., 2000; Erkut and Glickman, 1997; Zografos & Davis, 1989; Batta & Chiu, 1988). The research conducted on this particular subject involves the development of bi-objective or dissimilar shortest-path formulations. These approaches are specifically designed to improve both the safety and efficiency of single-origin and destination transportation routes.

Moreover, considerable research has been dedicated to determining multi-stop delivery routes for the distribution of hazardous materials, referred to as Hazardous Materials Vehicle Routing Problems (HMVRP) (Zografos & Androutsopoulos, 2004; Pradhananga et al., 2014). A major feature of the HMVRP is that it involves the optimization of both business-related (e.g., distance) and transportation risk objectives. Zografos and Androutsopoulos (2004) introduced a bi-objective HazMat vehicle routing problem with time windows, aiming to minimize transportation costs and risk, the latter being measured by the expected population exposure. It is assumed that trucks move from one customer to another through the corresponding shortest-distance road paths. A sequential insertion algorithm was proposed, enhanced with the capability of relocating routed customers. Pradhananga et al. (2014) enhanced the work of Zografos and Androutsopoulos (2004) by considering multiple alternative Pareto-efficient road paths between any pair of stops. Hence, in addition to forming delivery routes, the problem involved the selection of paths between subsequent stops. They proposed a multi-objective Ant Colony Optimization algorithm for solving the emerging bi-objective vehicle routing and scheduling problem. Wang et al. (2017) introduced an additional safety constraint to avoid the

domino effect in case of an accident. They studied a bi-objective hazardous materials vehicle routing problem in which the delivery vehicles are forbidden to simultaneously move in the same road path. The risk of any solution was expressed by the maximum routes' risk value instead of the sum of the routes' risk. The emerging bi-objective routing problem was solved by applying the ε-constraint technique, utilizing a big TSP route heuristic algorithm for large-scale problems. Zhang et al. (2018) provided a refined risk model that incorporates the effect of the load of the truck on the potentially impacted area in the event of an accident. The emerging HazMat Vehicle Routing problem aims at minimizing the transportation cost and the maximum route risk. It was solved by applying the ε-constraint method. Large-scale instances were solved by a big TSP route heuristic. Along this line, Bula et al. (2019) model transportation risk as a piecewise linear function of the load of the truck. They incorporate this model in a heterogeneous bi-objective vehicle routing problem and propose two solution algorithms: a multi-objective neighborhood dominance-based algorithm and an ε-constraint meta-heuristic. Men et al. (2020) addressed the inherent uncertainty associated with transportation risk by considering different scenarios for the HazMat release probability on any transportation link in case of an accident. They proposed a robust optimization model for the multi-objective vehicle routing problem with time windows that simultaneously minimizes the number of vehicles and the transportation risk. They additionally proposed a hybrid evolutionary algorithm for addressing the emerging robust counterpart. Chai et al. (2023) provided an Analytic Hierarchy Process based model that assesses the driving risk associated with a driver, taking into account his driving habits and personal characteristics (e.g., age, gender, etc.). Moreover, they incorporate the assignment of drivers to trucks into the bi-objective HazMat vehicle routing problem. They additionally provide a non-dominated genetic algorithm (NSGA-II) for solving the emerging bi-objective vehicle routing problem.

Finally, the class of HMVRPs has been enhanced with multi-depot vehicle routing problems mostly arising in the waste collection systems, wherein multiple waste processing units may be involved. Araee et al. (2020) studied the multi-depot vehicle routing problem for collecting and moving hazardous waste from the facilities producing the waste to the available depots (processing units). Various economic, social, and risk objectives are incorporated. The MOPSO and NSGA-II algorithms are employed to address the emerging multi-objective problem. Zhang et al. (2023) enhance the HMVRP by allowing trucks to visit multiple depots hence modeling the emerging problem as a bi-objective multi-depot heterogeneous vehicle routing problem with time windows. In this work, each depot has a certain capacity of HazMat. Transportation risk is assumed load-dependent. They proposed a multi-objective hybrid genetic algorithm for solving the problem.

The vast majority of the research on HMVRPs assumes transportation risk as the expected consequences of an accident, computed by the product of the probability of an accident times the potential (usually worst-case) consequences (e.g., population exposed). This classic definition of risk i.e. in Erkut and Verter (1998) where risk is defined as the product of the probability of an incident occurrence and the related population exposure, falls short in capturing the fact that not all potentially affected areas (and the residing population) stay at risk for the same time duration, especially in urban regions. In this work, we enhance the transportation risk definition by incorporating the time duration that the population stays at risk (i.e., lies within the area of impact of a HazMat accident). The time duration of the population

exposed at risk depends on two major factors: i) the travel speed of the truck (the higher the speed the lower the time duration that a resident remains within the potentially impacted area) Niu and Ukkusuri (2020), after studying real-life data, also conclude that the average speed of the vehicle has a significant impact on the non-accident mileage, similarly Wang et al. (2024) have established a correlation between average vehicle speed and accident risk. and ii) the load of the truck, i.e., the larger the load of the truck, the larger the size of the potential impacted area. As travel speeds are assumed to be time-dependent (in this work), the transportation risk measure under consideration is time and load-dependent.

Moreover, this work introduces a feature of Hazardous Materials distribution not previously addressed, concerning the effect of the schedule of the loading activities of the trucks at the depot on the routing decisions. The process of loading the trucks with the requested quantity of hazardous materials is carried out at the depot, using one or more loading facilities/positions. When the number of trucks waiting to get loaded exceeds the number of available loading facilities, the dispatcher confronts a scheduling problem in which he/she has to assign each truck to a loading facility for a certain time period (needed for performing the corresponding loading activity). However, the allocation of loading facilities to trucks has a direct effect on the earliest departure time of each truck route, a parameter that may severely affect the proposed (time-dependent) risk value of the route.

The work presented in this paper provides a bi-objective time-dependent vehicle routing and scheduling problem that aims to minimize the traveled distance and the total time duration of the population exposure due to hazardous materials shipments (risk metric). In addition to determining delivery routes, the proposed problem aims to provide the schedule of the corresponding loading activities. An NSGA-II (Non-dominated Sorting Genetic Algorithm II) algorithm with various novel features has been developed to address the proposed problem.

The remainder of this paper includes four sections. Section two discusses the major features of the proposed Hazardous Materials Vehicle Routing and Scheduling Problem. Section three presents the heuristic algorithm developed to address the proposed problem. In section four, we provide and discuss our computational experiments and results. Finally, in section five, we provide concluding remarks and outline future research directions.

2. Problem Definition

We assume a set of customers' orders for a given Hazardous Material. Each order i involves quantity w_i. The service time of customer i is denoted by t_i^s. The orders are serviced by a heterogeneous fleet of trucks $v \in V$ located in a single depot. Each truck has a capacity of Q_v. The objective of the problem is to determine a set of truck routes starting and terminating at the depot under the following constraints:

- Each order is delivered by a single truck through a single visit.
- Each truck is used at most once.
- The trucks move between stops (i.e., customers' premises and the depot) through the shortest-distance roadway paths.
- The trucks start their route at the depot and return to it within the time window $[a_o, b_o]$.

The ordered quantities are loaded on the trucks within the day of delivery through a limited number ξ of loading positions/stations located at the depot. Each loading position can serve up to one truck at a time with a fixed flow rate ρ. Each truck is served entirely by a single loading position. When the number of trucks needed is higher than the number of loading positions, a scheduling problem arises involving the allocation of every engaged truck to a single loading position for a period of time, referred to as *loading time*. To facilitate the allocation of trucks to loading positions, the daily time horizon is partitioned into a set of time intervals L of equal length γ (e.g., 10 minutes), called time slots. Depending on the load assigned to a truck, the corresponding loading activity might last for one or more time slots. In general, if a loading activity of a vehicle requires a loading time t, then it engages the loading station for $\left\lceil \frac{t}{t_s} \right\rceil$ time slots. For instance, if each time slot is 10 minutes long and a loading station requires one slot for loading 1.000 lt of a HazMat liquid, then a shipment of 3.500 would engage the loading station for 35 minutes or 4 slots. The finish time of any loading activity designates the earliest departure time of the corresponding truck. Hence, there is an interplay between the scheduling problem of the loading activities and the routing problem, since the risk performance of a truck route depends on the departure time of the truck (i.e., the proposed risk metric is time-dependent).

The proposed HazMat routing problem aims to simultaneously schedule the loading activities of the delivery and determine the truck routes so that the total travel distance and the total transportation risk are minimized.

2.1 Definition of Exposure Duration Metric

In this work, transportation risk is expressed by the duration that the population stays in danger due to a Hazardous Materials shipment passing nearby. Along this line, we define transportation risk as the aggregate exposure time of the members of the population exposed to the danger emanating from a given HazMat shipment, i.e., the sum of the exposure duration over all members of the potentially impacted population.

The transportation risk along a road path P_{ij} connecting any two stops (customers/depot) i and j, is equal to the sum of the risk metric values over the constituent road segments of the path, i.e., $P_{ij} = \{(g_0, g_1), (g_1, g_2), \dots, (g_{n-1}, g_n)\}$, where $g_0 = i$ and $g_n = j$. We assume that any truck carrying hazardous materials through any of these road segments sets at risk the population lying within a square area around the position of the truck (the truck is located in the middle of the square). It is worth noticing that the impact area around the HazMat vehicle is modeled by a square area rather than a circular area, as commonly used in relevant studies, i.e., Erkut and Verter (1998). While a circular representation provides a more accurate depiction of the potential impact zone, the square area representation simplifies the mathematical formulation of the problem. In addition, this simplification reduces computational complexity, especially in route optimization algorithms. Moreover, the square impact area is greater than that of a circle, which amplifies the significance of the HazMat risk. The size of the potential square impacted area depends on the type and the quantity of the transported hazardous material. Any single person in the population around the road segment is exposed to the risk associated with the HazMat shipment traversing that segment for as long

as he/she remains within the corresponding square (potentially impacted) area. Hence, the aggregate exposure time over the traversed segment is the sum of the exposure times of the entire population that stays for some time within this moving square area.

For instance, assume a HazMat shipment that traverses a roadway segment of length 1 km with a travel speed of 30 km/h and the side of the square impacted area around the truck is 200 m. (i.e., 200mx200m or 40,000 m^2). If the population density around the road segment is uniform and equal to 0.2 persons per m^2, then the population within the square impacted area is 4,000 persons (irrespective of the position of the truck on the segment). As the truck traverses the road segment, the impacted area around it moves along as well. Hence, any person located in a zone of width 200 m around the segment will remain within the impacted area for the time period that it takes for the truck to travel 200 m (i.e., 24 sec or 0.4 minutes). The total population along the road segment that will be exposed at some point in time is equal to (200x1000)x0.2 or 40,000 persons. Hence, the total population exposure duration is equal to (40,000 persons x 0.4 minutes) or 16,000 person-minutes. It is evident that the proposed risk metric depends on the travel speed of the truck (i.e., the faster the truck moves along a roadway segment, the less time each resident stays within the area of impact) and the size of the impact area.

It is worth noticing that the travel speed in the example above was assumed constant throughout the link (for the sake of simplicity). However, in this work the travel speed on any road segment (g_k, g_{k+1}) of length $d_{g_k g_{k+1}}$, is assumed time-dependent, modelled as a step function of the departure time from the upstream node g_k. The daily time horizon is partitioned into time periods $[\tau_h, \tau_{h+1}]$ for $h = 0,1, \dots, m-1$, for which the average travel speed in any roadway segment (g_k, g_{k+1}) is $u_{g_k g_{k+1} h}$. Thus, the travel speed $u_{g_k g_{k+1}}(\tau)$ on segment (g_k, g_{k+1}) when the truck departs from g_k at time $\tau \epsilon [\tau_h, \tau_{h+1}]$ is equal to $u_{g_k g_{k+1} h}$ and the travel time on (g_k, g_{k+1}) is computed by equation (1),

$$tt_{g_k g_{k+1}}(\tau) = \frac{d_{g_k g_{k+1}}}{u_{g_k g_{k+1} h}}, \ \tau \epsilon [\tau_h, \tau_{h+1}] \ \text{for } h = 0,1, \dots, m-1 \tag{1}$$

where τ represents the departure time from the upstream node g_k.

The size of the square (potentially) impacted area is fully determined by the length of its side. Given a shipment of HazMat type ζ and quantity w, the length $r(w, \zeta)$ of the side of the relevant square impacted area around the shipment is defined by the piecewise linear function (2). Parameter $r^o_{\delta t \zeta}$ is constant and parameter $a_{\delta t \zeta}$ expresses the rate of change of the length of the side of the impacted area with respect to the shipment weight and type of HazMat.

$$r(w,t) = r^o_{\delta t \zeta} + a_{\delta t \zeta} \cdot (w - w_\delta), \ \ w \in [\beta_\delta, \beta_{\delta+1}], \delta = 0, \dots, |\Delta| - 1. \tag{2}$$

We now define the proposed risk metric associated with a HazMat shipment of type ζ and weight w traversing a roadway segment (g_k, g_{k+1}). Figure 1 illustrates such a case. It is assumed that the truck departs from g_k at time τ. The impacted area moves along the segment accompanying the truck movement with travel speed denoted by $u_{g_k, g_{k+1}}(\tau)$. The average population density around (g_k, g_{k+1}) is denoted by $pop_{g_k, g_{k+1}}$.

We assume a marginal area section (as described in Figure 1) vertical to (g_k, g_{k+1}), with width Δx and length equal to $r(w, \zeta)$ (or r for simplicity).

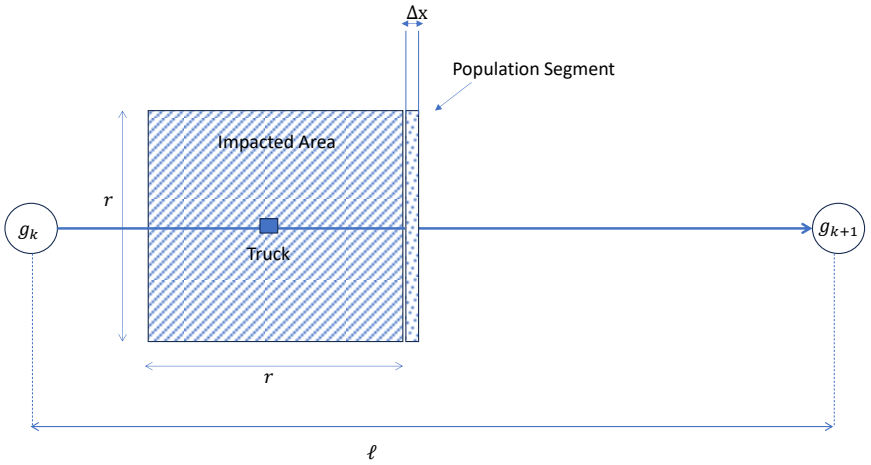

Fig. 1: Representation of the impacted area when a truck traverses the roadway segment (g_k, g_{k+1}).

Figure 2 presents two snapshots from the truck's traversal over (g_k, g_{k+1}) at the following points in time: i) when the impacted area around the truck starts to cover the area marginal section (top of Fig. 2), and ii) when the marginal area section gets out of the coverage from the truck's impacted area (bottom of Fig. 2). It is evident (Fig. 2) that the marginal area section will lie within the truck's impacted area while the truck will be moving along (g_k, g_{k+1}) from position A until it reaches position B, covering a distance of length $r(w, \zeta)$.

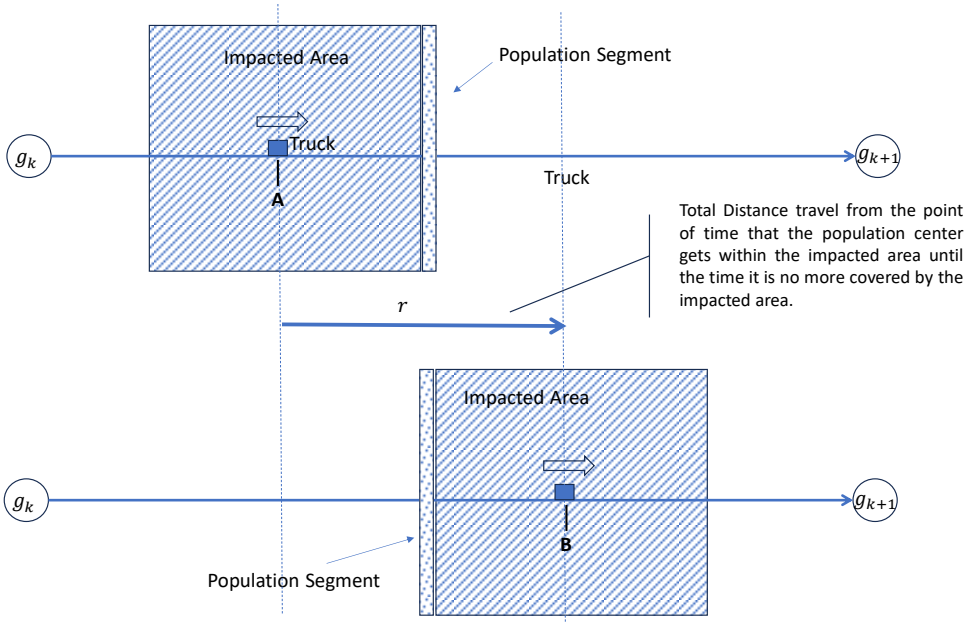

Fig. 2: Representation of two snapshots of the impacted area when the truck traverses the segment (g_k, g_{k+1}).

Hence, if Δx is small enough, any member of the population within this marginal area section will be exposed to the risk of the HazMat shipment carried by the truck for a duration equal to

($\frac{r(w,\zeta)}{u_{g_k g_{k+1}}(\tau)}$). The total duration of the population exposure within this marginal area section is equal to the product of the total population in the section (i.e., $pop_{ij} \cdot (r(w,\zeta) \cdot \Delta x)$) with the duration of exposure per population member. Equation (3) presents the total exposure time of the population around link (g_k, g_{k+1}).

$$R_{g_k g_{k+1}}(\tau, w, \zeta) = \int_0^{\lambda} \frac{r(w,\zeta)}{u_{g_k g_{k+1}}(\tau)} \cdot pop_{ij} \cdot r(w,\zeta) dx \quad (3)$$

By moving out of the integral all the parameters that do not depend on the position of the truck, equation (4) is derived.

$$R_{g_k g_{k+1}}(\tau, w, \zeta) = \frac{r(w,\zeta)}{u_{g_k g_{k+1}}(\tau)} pop_{ij} \cdot r(w,\zeta) \int_0^{\ell} dx \quad (4)$$

The integral is equal to ℓ, leading to equation (5).

$$R_{g_k g_{k+1}}(\tau, w, \zeta) = r^2(w,\zeta) \cdot pop_{ij} \cdot \frac{\ell}{u_{g_k g_{+1}}(\tau)} \quad (5)$$

Finally, given that the ratio $\frac{\ell}{u_{g_k g_{k+1}}(\tau)}$ expresses the travel time on the segment (g_k, g_{k+1}) we get the formula (6) for the proposed transportation risk measure on the segment (g_k, g_{k+1}).

$$R_{g_k g_{k+1}}(\tau, w, \zeta) = r^2(w,\zeta) \cdot pop_{g_k g_{k+1}} \cdot tt_{g_k g_{k+1}}(\tau) \quad (6)$$

The corresponding transportation risk $R_{P_{ij}}(\tau, w, \zeta)$ of a HazMat type ζ and weight w departing from the upstream stop i at time τ_i on a path P_{ij} is given by formula (7).

$$R_{P_{ij}}(\tau, w, \zeta) = \sum_{k=0}^{n-1} R_{g_k g_{k+1}}(\tau_{g_k}, w, \zeta) \quad (7)$$

Where $\tau_{g_0} = \tau$, and $\tau_{g_k} = \tau_{g_{k-1}} + tt_{g_{k-1} g_k}(\tau_{g_{k-1}})$, for $k = 1, \dots, n$

Henceforth, the proposed risk metric will be referred to as the *Population Aggregate Exposure Duration.*

2.3 Mathematical Formulation

The proposed problem has been formulated as a Mixed Integer Linear Programming (MILP) model. The problem is defined in a graph $G(N, A)$ where N is the set of nodes representing the customers' locations, the point of origin 0 and the point of destination $n + 1$, both referring to the depot and A is the set of arcs (i, j) representing the travel from node i to node j. To facilitate the formulation, the time horizon of the problem is discretized to a set of time units (e.g., 5 minutes) denoted by T and the travel time of a truck on arc $(i, j) \in N$ departing from node i at time $\tau \in T$ is denoted by $tt_{ij\tau}$. Moreover, we assume that $tt_{ij\tau}$ is an integer multiple of the time

unit used. The variables used for the model formulation are presented and explained in the table below (table 1).

Decision Variables
$x_{ijv\tau} \in \{0,1\}, (i,j) \in A, v \in V, \tau \in T,$ if $x_{ijv\tau} = 1$ then vehicle v departs from stop i heading to j at time $\tau \in T$,
$y_{0v} \geq 0, v \in V$, departure time from the depot for vehicle v
$y_{(n+1)v} \geq 0, v \in V$, return time to the depot for vehicle v
$y_{iv} \geq 0, i \in N \backslash \{0, n+1\}, v \in V$ departure time of vehicle v from the customer i
$\sigma_{vl} \in \{0,1\}, v \in V, l \in L,$ if $\sigma_{vl} = 1$ then the vehicle v starts to get service (loading process starts) at slot $l \in L$
$z_{vl} \in \{0,1\}, v \in V, l \in L$, if $z_{vl} = 1$ then the vehicle v is still under service (is being loaded) during slot $l \in L$
$S_{vl} \in \{0,1\}, v \in V, l \in L$, if $S_{vl} = 1$ then the loading of vehicle v has started before or during slot l
$F_{vl} \in \{0,1\}, v \in V, l \in L$, if $F_{vl} = 1$ then the loading of vehicle v has been completed before slot l
$w_{iv\tau} \geq 0, i \in N \backslash \{n+1\}, v \in V, \tau \in T$, the quantity of the load on vehicle v when it leaves stop i
$u_{ijv\tau} \geq 0, (i,j) \in A, v \in V, \tau \in T$, the quantity of the load on vehicle v when it traverses arc $(i,j) \in A$
$f^L_{ijv\delta\tau} \in \{0,1\}, (i,j) \in A, v \in V, \tau \in T, \delta = 0, \dots, \lvert\Delta\rvert - 1,$ if $f^L_{ijv\delta\tau}$=1 then the quantity of the load of truck v (i.e., $u_{ijv\tau}$) as it traverses arc (i,j) is below β_δ
$f^c_{ijv\delta\tau} \in \{0,1\}, (i,j) \in A, v \in V, \tau \in T, \delta = 0, \dots, \lvert\Delta\rvert - 1$, if $f^c_{ijv\delta\tau}$=1 then $u_{ijv\tau} \in [\beta_\delta, \beta_{\delta+1})$
$f^u_{ijv\delta\tau} \in \{0,1\}, (i,j) \in A, v \in V, \tau \in T, \delta = 0, \dots, \lvert\Delta\rvert - 1$, if $f^u_{ijv\delta\tau} = 1$ then $u_{ijv\tau} \geq \beta_\delta$

Table 1: Decision variables used in the model formulation.

The mathematical formulation of the problem is expressed by (8)-(35). The proposed model contains two objective functions. Objective function (8) expresses the total traveled distance whereas objective function (9) expresses the HazMat risk. The trade-off between the two objectives of the MILP formulation introduced above is evaluated and presented in Appendix A.

Objective function 1 (Distance)

$$Min\left(\sum_v \sum_{i,j}\left(\sum_\tau x_{ijv\tau} \cdot d_{ij}\right)\right) \quad (8)$$

Objective function 2 (Risk)

$$Min\left(\sum_\tau \sum_v \sum_{i,j}\left(\sum_\delta f^c_{ijv\delta\tau} \cdot {r_\delta}^2\right) \cdot tt_{ij\tau} \cdot pop_{ij}\right) \quad (9)$$

Constraint (10) implies that each customer is visited by a single vehicle exactly once. Constraint (11) indicates that if vehicle v arrives at customer i then the same vehicle should

service and leave from i. Constraint (12) defines that if a truck starts from node 0 (depot) it must return to node $n+1$ (depot).

$$\sum_{i\in N\setminus\{n+1\}}\sum_{v}\sum_{\tau} x_{ijv\tau} = 1 \;\forall\, j \in N\setminus\{0, n+1\} \quad (10)$$

$$\sum_{j}\sum_{\tau} x_{jiv\tau} - \sum_{j}\sum_{\tau} x_{ijv\tau} = 0 \;\forall\, i \in N\setminus\{0, n+1\}, v\in V \quad (11)$$

$$\sum_{j\in N\setminus\{0\}}\sum_{\tau} x_{0jv\tau} - \sum_{i\in N\setminus\{n+1\}}\sum_{\tau} x_{in+1v\tau} = 0 \quad \forall\, v \in V \quad (12)$$

Constraints (13) to (15) are used as flow conservation constraints. In detail, constraint (13) implies that if a vehicle departs from a customer i at time τ, it should have left from the previous stop at $\tau_k{}'$. Constraints (14) and (15) imply that the load of the truck entering a customer minus the load of the truck upon leaving the customer must be equal to the ordered quantity of the customer.

$$\sum_{k\in N\setminus\{n+1\}} x_{kiv\tau_k{}'} - \sum_{j\in N\setminus\{0\}} x_{ijv\tau} = 0\ ,\ \forall\, N\setminus\{0, n+1\}, v\ \in V, \tau\in T,\ \tau_k{}' = \tau - t_i^s - tt_{ki\tau} \quad (13)$$

$$w_{iv\tau} - w_{jv\tau'} + \left(1 - x_{ijv\tau}\right)\cdot M \geq q_j \quad \forall\,(i,j)\ \in N\setminus\{n+1\}, v\in V, \tau\in T,\ \tau\ {}' = \tau + tt_{ij\tau} + t_j^s \quad (14)$$

$$\sum_{i\in N/\{n+1\}}\sum_{v}\sum_{\tau} u_{ijvt} - \sum_{i\in N/\{n+1\}}\sum_{v}\sum_{\tau} u_{jivt} = q_j \quad \forall\ j\ \in N\setminus\{0, n+1\} \quad (15)$$

Constraint (16) states that the load of a truck traversing any link of the network should not exceed its capacity. In addition, it implies that if a link (i,j) isn't traversed by vehicle v at time τ then no HazMat quantity is carried by vehicle v at time τ across the link (i,j) (i.e., $u_{ijv\tau}$ is forced to 0). Constraint (17) indicates that the truckload on an arc (i,j) is equal to the load of the truck upon leaving i. Constraint (18) implies that all trucks return to the depot $(n+1)$ empty.

$$u_{ijv\tau} \leq x_{ijv\tau}\cdot Q_v \quad \forall\,(i,j)\in A, v\in V, \tau\in T \quad (16)$$

$$\sum_{j\in N\setminus\{0\}} u_{ijv\tau} = w_{iv\tau} \;\forall\, i\in N\setminus\{n+1\}, v\in V, \tau\in T \quad (17)$$

$$\sum_{\tau}\sum_{i\in N/\{n+1\}} u_{i(n+1)v\tau} = 0 \;\forall\; v\in V \quad (18)$$

Constraints (19) to (28) relate to scheduling the loading operations at the depot. In detail, constraint (19) indicates that every truck gets a starting loading slot at the depot. Constraint (20) indicates no more than ξ trucks can be serviced in parallel during any slot $l\in L$. Constraints (21) and (22) imply that the total number of slots allocated to servicing truck v should cover the corresponding loading duration required to load the truck (with the total volume $\left(\sum_{\tau} w_{0v\tau}\right)$ allocated to v). Note that M denotes a very large number. Constraints (23) to (26) determine the consecutive slots allocated for loading any truck v. Constraint (27) ensures that the departure time of a truck from the depot coincides with the time that its loading operation terminates. Note that e_l denotes the point in time that the corresponding slot interval l begins. Constraint (28) forces the departure of each truck from the depot to occur within the time window $[a_o,\ b_o]$.

$$\sum_{l}\sigma_{vl} = 1 \quad \forall\ v\in V \quad (19)$$

$$\sum_{v} z_{vl} \leq \xi \quad \forall\, l\in L \quad (20)$$

$(1-\sigma_{vl})\cdot M+(\sum_{s=l}^{|L|} z_{vs})\cdot \gamma \geq \left(\sum_{\tau}\ w_{0v\tau}\right)\cdot \rho\ \ , \forall\ l \in L, v \in V$ (21)

$(1-\sigma_{vl})\cdot M+(\sum_{\tau}\ w_{0v\tau})\cdot \rho \geq \left[\left(\sum_{s=l}^{|L|} z_{vs}\right)\cdot \gamma\right]-1\ \ \forall\ l \in L, v \in V$ (22)

$S_{vl}=\sum_{s=0}^{l}\sigma_{vl}\ \ \forall\ v \in V, l \in L$ (23)

$\sum_{s=0}^{l}\sigma_{vl} \geq F_{vl}\ \ \forall\ \ v \in V, l \in L$ (24)

$F_{v(l+1)} \geq F_{vl}\quad \forall\ v \in V, l = 0, \dots, |\ L|-1$ (25)

$z_{vl}=S_{vl}-F_{vl}\quad \forall\ v \in V, l \in L$ (26)

$y_{0v}=\sum_{l=0}^{|L|}\sigma_{vl}\cdot\ e_l+\left(\sum_{l}\ z_{vl}\cdot\gamma\right)\ \ \forall\ \ v \in V$ (27)

$a_o \leq y_{0v} \leq b_o\ \ \forall\ \ v \in V$ (28)

Constraints (29) to (35) are used to determine the interval $[\beta_\delta, \beta_{\delta+1})$ that the load carried by a truck falls in as it traverses link (i, j). Constraints (29) and (30) imply that for any load value and any interval $[\beta_\delta, \beta_{\delta+1})$ one of the variables $f^L_{ijv\delta\tau}, f^c_{ijv\delta\tau}, f^u_{ijv\delta\tau}$ should be equal to one. Note that M_2 denotes a large number. Constraints (31) and (32) imply that if $u_{ijv\tau}$ is higher than or equal to β_δ then $f^L_{ijv\delta\tau}$ must be equal to 0. Similarly, constraints (33) and (34) imply that if $u_{ijv\tau}$ is higher than $\beta_{\delta+1}$ then $f^U_{ijv\delta\tau}$ must be equal to 1. Constraint (35) implies that if vehicle v does not traverse the link (i, j) at time τ, then $f^C_{ijvy\tau}$ should be equal to zero for any δ.

$f^L_{ijv\delta\tau}+f^C_{ijv\delta\tau}+f^U_{ijv\delta\tau} \leq 1+\left(1-x_{ijv\tau}\right)\cdot M_2\ \ \forall\ i, j \in N, v \in V, \tau \in T, \delta = 0, \dots |\Delta|-1$ (29)

$\left(1-x_{ijv\tau}\right)\cdot M_2+f^L_{ijv\delta\tau}+f^C_{ijv\delta\tau}+f^U_{ijv\delta\tau} \geq 1\ \ \forall\ i, j \in N, v \in V, \tau \in T, \delta = 0, \dots |\Delta|-1$ (30)

$\left(1-x_{ijv\tau}\right)\cdot M_2+u_{ijv\tau}-\beta_\delta \geq -f^L_{ijv\delta\tau}\cdot M\ \ \forall\ i, j \in N, v \in V, \tau \in T, \delta = 0, \dots |\Delta|-1$ (31)

$\frac{1}{2}+u_{ijv\tau}-\beta_\delta \leq \left(1-f^L_{ijv\delta\tau}\right)\cdot M+\left(1-x_{ijv\tau}\right)\cdot M_2\ \ \forall\ i, j \in N, v \in V, \tau \in T, \delta = 0, \dots |\Delta|-1$ (32)

$\frac{1}{2}+u_{ijv\tau}-\beta_{\delta+1} \leq f^U_{ijv\delta\tau}\cdot M+\left(1-x_{ijv\tau}\right)\cdot M_2\ \ \forall\ i, j \in N, v \in V, \tau \in T, \delta = 0, \dots |\Delta|-1$ (33)

$\left(1-x_{ijv\tau}\right)\cdot M_2+u_{ijv\tau}-\beta_{\delta+1} \geq -\left(1-f^U_{ijv\delta\tau}\right)\cdot M\ \forall\ i, j \in N, v \in V, \tau \in T, \delta = 0, \dots |\Delta|-1$ (34)

$x_{ijv\tau} \geq \sum_{\delta=0}^{y=|\Delta|-1} f^C_{ijv\delta\tau}\ \forall\ i, j \in N, v \in V, \tau \in T$ (35)

3. Solution Algorithm

An NSGA-II algorithm (Non-dominated Sorting Genetic Algorithm II) (Deb et. al 2000 & 2002) has been developed to address the problem under study. NSGA-II is a genetic algorithm that uses a non-dominated sorting mechanism to rank solutions based on their Pareto dominance. The algorithm operates on a population of solutions and iteratively applies reproduction operators to generate new solutions. In the context of the proposed problem, the initial population is generated by a Reactive Grasp algorithm. Overall, the proposed algorithm

involves the following novel features: i) a new one-point reproduction (cross-over) operator, ii) a new multi-point reproduction operator aiming to enhance the diversity of the population created by the NSGA-II algorithm, and iii) the development of a post-optimization procedure that deals with scheduling the loading activities emerging from the truck routes determined. In addition, the risk is dynamically recalculated throughout the algorithm for all solutions generated, including those produced by the novel reproduction operators and the post-optimization procedures, as it depends on both the truck's load and its departure time from the depot, in alignment with the formulation detailed in Section 2.1. In what follows we present the main steps and the various components of the proposed algorithm.

3.1 Chromosomes and Genes

To facilitate the implementation of the proposed NSGA-II algorithm, any problem solution is represented by a list of tuples of the form (*vehicle id, customer id*), where *vehicle id* corresponds to the vehicle that services the customer associated with the *customer ID*. This structure is called a chromosome and each of the tuples is called a gene. Given a problem solution, its representation as a chromosome is built by concatenating the sequence of customers of the routes of the solution. Figure 3 provides an example that illustrates how a problem solution is transformed into a chromosome. For convenience, each chromosome is depicted by a matrix of two rows: the first row refers to the customer ID, and the second to the corresponding vehicle ID (each column represents a gene of the chromosome).

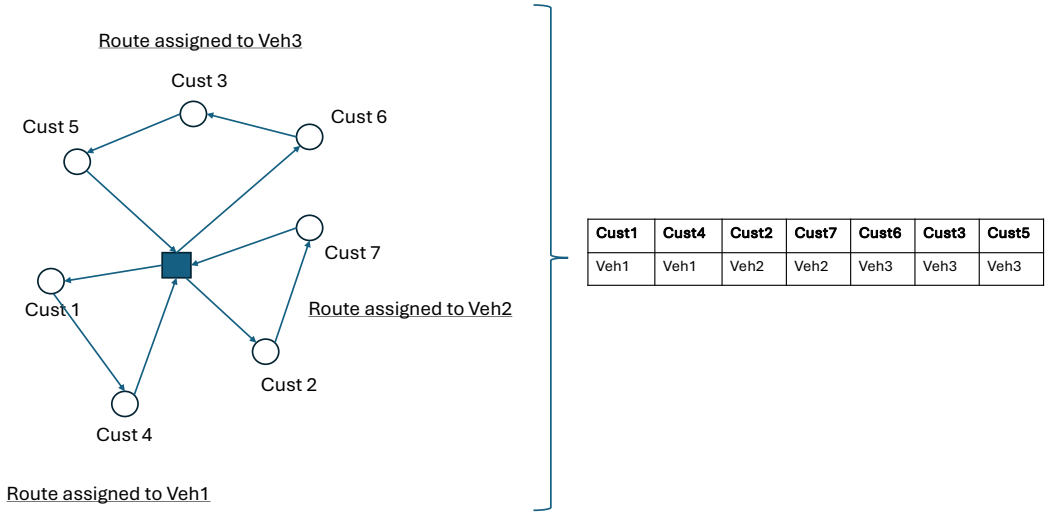

Cust1	Cust4	Cust2	Cust7	Cust6	Cust3	Cust5
Veh1	Veh1	Veh2	Veh2	Veh3	Veh3	Veh3

Fig. 3: Representation of a problem solution as a chromosome

3.2 Main Steps

The proposed NSGA-II algorithm involves the following steps, (the pseudocode is presented in Appendix B):

1. An initial population of N solutions is created using a Reactive Grasp algorithm.
2. A predefined number of iterations are performed in which:

- Step 2.1: An offspring population of size N is created out of the initial population by applying a reproduction operator.
- Step 2.2: The objective value (for each objective) of each solution is calculated.
- Step 2.3: The offsprings' population is merged with the parents' population. The solutions of the enhanced population are grouped to Pareto dominance fronts, i.e., solutions that are not dominated by any other solution are placed in the first group (front). The second front of non-dominated solutions is determined from the pool of the remaining solutions after removing those in the first front, etc.
- Step 2.4: The solutions belonging to the best k Pareto dominance fronts, are added to the final population until no more than N solutions are passed to the final population.
- Step 2.5: The $k+1$ Pareto front is selected and the crowding distance of each solution is calculated as per formula (36).
- Step 2.6: The best solutions in terms of crowding distance are sequentially selected and passed to the final population until its final size is equal to N.
- Step 2.7: Return to step 2 or terminate the algorithm when the stopping criterion of the maximum number of iterations is met.

A solution is said to be non-dominated if there is no other solution in the population that scores equal to or higher than it across all objectives. Hence, the Pareto dominance rank evaluates the quality of a solution by considering its dominance relationship with the other solutions in the population (i.e. the solutions in the 1st Pareto dominance front dominate the solutions to all the other fronts, the solutions of the 2nd front dominated the solutions to the remaining fronts, i.e., 3rd, 4th, etc.).

The crowding distance of a solution is a measure of the "crowdedness" of its neighboring solutions. A solution with a high crowding distance value is located in a neighborhood of solutions that are more diverse and spread out in the two-dimensional objective space. On the contrary, a solution with a low crowding distance value is located in a more dense neighborhood of solutions. The crowding distance (c_i) of a solution i is defined as the average distance between the solution and its neighboring solutions in the population, with respect to the different objectives being optimized. To compute this value, the solutions of the population are placed on M lists (M is the number of objective functions, in our case $M = 2$), each one ranked based on a different objective function. Then, for each solution i in the emerging sorted lists $m = 1,..,M$ (apart from the first and the last), the crowding distance as presented also by Deb et al. (2002) is determined by the following steps:

- Calculating the differences ($f_{i+1}^m - f_{i-1}^m$), where f_{i+1}^m is the value of solution $i+1$ (i.e., the one next to solution i in list m) under objective function m and f_{i-1}^m is the value of solution in the rank $i-1$ of the list m (i.e., the previous one to solution i) under objective function m
- Each of these differences is normalized by dividing them by the difference between the max and min values of the objective function ($f_{max}^m - f_{min}^m$)
- The normalized differences are then summed over all $m = 1,..M$. The purpose of crowding distance is to facilitate the algorithm to maintain a diverse set of non-dominated solutions.

$$c_i = \sum_{m=1}^{M} \frac{f_{i+1}^m - f_{i-1}^m}{f_{max}^m - f_{min}^m} \quad (36)$$

The reproduction phase of the algorithm is performed by three alternative operators: i) a one-point crossover operator, ii) a new multi-point crossover operator, and iii) a mutation operator supported by a binary tournament selection procedure. The emerging offspring are assessed in terms of feasibility. If infeasibilities are detected then two alternative processes are applied to obtain feasibility: i) the Relocation method, and ii) the Route Splitting method. In what follows we present the reproduction operators, the two chromosome feasibility methods and the Reactive Grasp used for producing the initial population.

3.3 One-Point Crossover

The basic idea of a crossover operator is to create new offspring solutions by exchanging genetic information (genes) between two parent solutions. Two parents are initially chosen and a crossover point that splits both parents into two parts is randomly selected (arrow in Figure 4). Given the structure of the chromosome (each gene involves linking a customer to a vehicle), a novel implementation of the one-point crossover operator is proposed, in which the vehicle ids of the genes of the parents are held in place. It is only the customers swapped between the genes of the parents.

In more detail, if the crossover point is right after gene k, then the customer ID of the hth gene for $h = n - k + 1$ up to n, of parent 1 will be changed to the customer ID of the corresponding hth gene of parent 2, if and only if this customer ID is not already present in one of the $(k + h - 1)$ genes of the offspring under development. To make sure that the emerging offspring includes all customers with no duplicates, we define a list Z_1 (or Z_2 for parent 2) that contains all customers of parent 1 included in genes $n - k + 1$ up to n. Every time the customer in gene h of the offspring is fixed it is removed from the list Z_1. By the end of building the offspring chromosome, Z_1 should be empty. The example that follows clarifies the crossover operator. As depicted in Figure 4, the crossover point is positioned immediately after the third gene. This implies that customers 2, 7, 3, and 6 from genes 4-7 of parent 2 are to be extracted and subsequently inserted into the corresponding genes 4-7 of parent 1. The list Z_1 is as follows: (5, 2, 6, 7) i.e., the customers currently contained in genes 4-7 of parent 1. It is worth noting that we only move the customers, not the entire genes. Hence, gene 4 of chromosome 1 (Fig. 4) will still contain Veh2, but customer 5 will be considered to be replaced by customer 2. A verification process is conducted to determine whether customer 2 is already present in the preceding genes of the partial offspring. Given that the customer is not present in prior genes, the customer is subsequently inserted into the fourth gene of the partial offspring chromosome. Z_1 is updated to: (5, 6, 7), i.e. customer 2 is removed from Z_1. Similarly, customer 7 does not exist in any earlier positions of offspring 1, and therefore it replaces customer 2 in the 5th gene. Z_1 is updated to: (5, 6). However, in the 6th gene of offspring chromosome 1, customer 3 cannot replace customer 6, since it is already present in the 3rd gene. In this case, the customer of the 6th gene (i.e., customer 6) is not replaced. Given that Customer 6 is not present in any of the previous genes, it remains in place. Z_1 is updated to: (5). Finally, customer

6 cannot replace customer 7 in the final (7^{th}) gene. Moreover, customer 7 cannot remain in place since it is already present in the 5^{th} gene. In this case, the initial step involves identifying the first available customer in list Z_1 who has not been present in any of the previous genes (i.e., customer 5). Subsequently, this customer is placed in the 7^{th} gene. A similar procedure is executed for parent 2. Through this reproductive process, two offspring are generated from a pair of parents (Fig. 4).

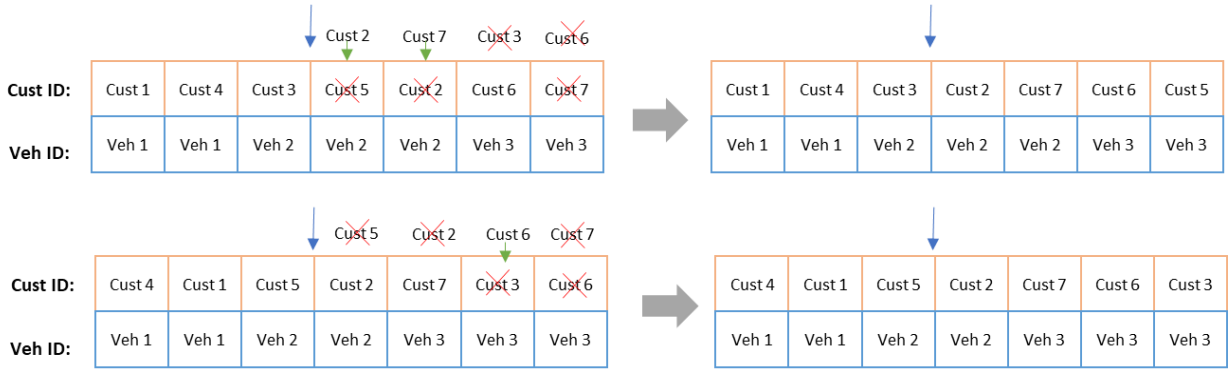

Fig. 4: Example of the One-Point Crossover

3.4 Multi-Point Crossover Operator

A new Multi-Point Crossover Operator has been developed as an alternative procedure to the one-point crossover operator. The objective of this technique is to have a better mix of the parent chromosomes for developing two offspring substantially different from the parents. We outline the proposed Multi-Point Crossover Operator and present a visual representation of how the offsprings are built (Figure 5). The proposed operator involves the following steps:

- Start with Parent 1 and copy the top a% (e.g., 40%) of the genes to the offspring, where a is a random number, e.g., customers 2, 4, 5, 6 (underlined) in Fig. 5.
- Go to Parent 2 and find the location of the last inserted gene as per the previous step i.e. customer 6, and then copy to the offspring the β% (e.g., 30%) of the genes after the specific location which are not already in the offspring i.e. customers 1, 3 and 10.
- Go back to Parent 1 find the location of the last inserted individual i.e. customer 10 (underlined), and then copy to the offspring the γ% (e.g. γ=10%) of the remaining unused genes (positioned after the specific location) which have not been already inserted to the offspring i.e. customer 8.
- Go to Parent 2 and find the location of the last inserted gene i.e. customer 8, and after that add all the remaining unused genes to the offspring i.e. customers 9 and 7.

The above steps create the first offspring out of two parents. Replicating this procedure starting from Parent 2 this time,

and then continue with Parent 1 in step 2 and so on, would lead to the second offspring.

As depicted in Figure 5, each customer is paired with a vehicle. In the Multi-Point Crossover Operator, both the customer and its connected vehicle are transferred to the offspring. Initially, the offspring may not be feasible. However, the feasibility of the offspring is subsequently attained using the methods described in the following subsections.

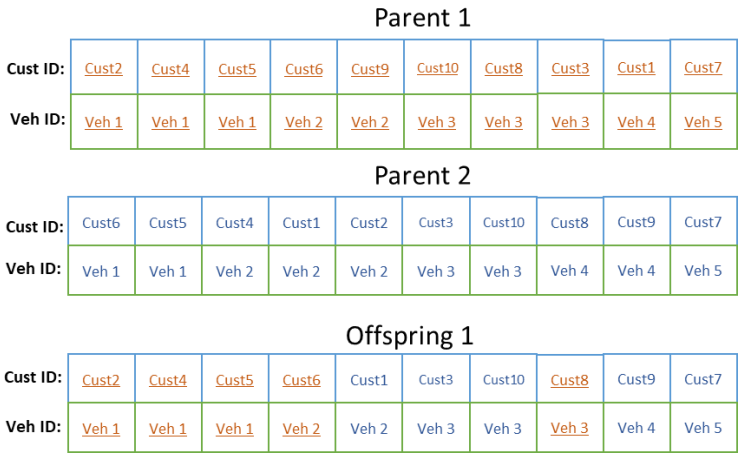

Fig. 5: Example of the new Multi-Point Crossover operator.

3.5 Mutation

The selection of the chromosomes for mutation is performed through a binary tournament. It is a simple and efficient selection scheme that involves randomly picking two individuals from the population and comparing the values of their objective functions to determine which one is better. In detail, the values of the objective functions of the two individuals are compared and the winner is selected while the loser is no longer a candidate to produce an offspring. In the case of a tie (i.e. non non-dominated solutions), a chromosome is randomly selected. The winning chromosome goes through mutation, which applies random changes in the chromosome. In this work, the mutation involves the exchange of customers between two randomly selected genes.

3.6 Feasibility Methods

A common feature of the reproduction operators is that the emerging offspring solutions may violate the capacity constraint of one or more trucks. To detect any capacity violation, the chromosome is decomposed to truck routes. This is straightforward since each gene of the chromosome involves: a customer ID and the ID of the truck it has been assigned to. Moreover, the sequence of customers per route is identical to the sequence of the corresponding genes in the chromosome. Each of the emerging truck routes is then checked for any capacity violation. If a violation is found, then one of the following two routines is applied: i) Customer Relocation, and ii) Route Splitting.

3.6.1 Customer Relocation

This routine tries to relocate the customers of a capacity infeasible route to the first available truck that has sufficient capacity to accommodate the customer under consideration. The relocation search stops when one of the customers can be feasibly relocated to another route. The position of the relocated customer in the identified route is determined by a sorting technique that determines the alternative candidate positions along the route that may result in a non-dominated solution. Then the routine randomly chooses one of the alternative positions to serve as the optimal relocation position for the customer under consideration.

The aforementioned procedure is iteratively executed for every single truck. If a capacity violation cannot be resolved by relocation, we initiate a corrective procedure. In detail, the first half of the customers already assigned to the route are removed. This ensures that the route's capacity constraints are adhered to and paves the way for creating feasible routes. Subsequently, the assignment process restarts, allowing for the creation of revised, compliant routes. The corrective procedure can be repeated as many times as needed until a feasible solution is provided.

Figure 6 illustrates an example in which a chromosome is mutated, resulting in an offspring that violates the capacity constraint. In particular, the total quantity assigned to vehicle 2 exceeds its capacity. By using the above presented method, the first customer of vehicle 2 is relocated to vehicle 3. The pseudocode is also presented in Appendix C.

Fig. 6: Representation of creating feasible solutions using the Customer Relocation Method.

3.6.2 Route Splitting

We have also created a split procedure that treats the sorted list of customers of an offspring as a large TSP route and breaks it down to truck routes forming a new solution (chromosome). The split method ignores the assignment of customers to trucks that are stored as vehicle IDs in the genes of the chromosome. This routine iteratively selects a truck from the top of the list of vehicles V (sorted in descending order of their capacity) and assigns the largest possible first segment of the TSP route that does not violate the capacity of the selected truck. Both the truck and the customers are removed from list V and the TSP route respectively, and the process is repeated. This process is iterated as long as the TSP route remains non-empty.

3.7 Generating the Initial Population

The proposed Reactive GRASP (Jaikishan & Patil, 2019) algorithm generates the initial population of solutions through a semi-random insertion heuristic that uses candidate lists of customers (Marinakis et al., 2007; Moura & Oliveira, 2009). The main idea is to rank the unrouted customers based on different metrics and create one sorted list of customers per

metric. The higher a customer is positioned in these lists, the higher the probability of being the next one to be selected and routed. An overall priority index is developed for each customer combining its position in each of the lists. In this work, we create three sorted lists by sorting the unrouted customers under three metrics: i) the customer's order quantity, ii) the population density in the area of the customer's premises, and iii) the proximity of the customer's premises to the last routed customer.

In what follows, we outline the steps of the insertion procedure in an iteration η of the procedure.

i. A customer is semi-randomly selected from the set of v_u unrouted customers, through a random wheel experiment. The selection probabilities of the customers are calculated as follows:

a. The v_u unrouted customers are placed in three different lists sorted in each one as follows:

- List 1: The unrouted customers are sorted in descending order of the requested quantity. Then the customer i ranked at the k^{th} position in List 1 is assigned a priority weight denoted by z_{1i}^{η}, equal to $(v_u - k)$. For example, in a sorted list of ten customers, the one at the top of the list is assigned a priority weight of 9, the next customer in line is assigned 8, and so forth.
- List 2: The unrouted customers are sorted in ascending order based on the population density of the area around their location. Similarly, a priority weight (denoted by z_{2i}^{η}) of $(v_u - k)$ is assigned to customer i at $the\ k^{th}$ position in List 2,
- List 3: The unrouted customers are sorted in ascending order based on their proximity to the customer last included in a route (or the depot if the route is empty). A priority weight (denoted by z_{3i}^{η}) of $(v_u - k)$ is assigned to customer i at the k^{th} position in List 3. This list differs from the previous two as it gets updated in every iteration of the procedure (since the last customer of the route under construction might change). If the route is empty, then proximity from the depot is used. It is this last metric that justifies the term "reactive" used to characterize the proposed GRASP algorithm.

b. An overall priority (ε_i^{η}) is assigned to customer i, computed by the weighted sum of the corresponding priority weights ($z_{1i}^{\eta}, z_{2i}^{\eta}, z_{3i}^{\eta}$),

$$\varepsilon_i^{\eta} = \pi_1 \cdot z_{1i}^{\eta} + \pi_2 \cdot z_{2i}^{\eta} + \pi_3 \cdot z_{3i}^{\eta}$$

where $\pi_1 + \pi_2 + \pi_3 = 1$ and they are randomly selected to enhance the randomization of the algorithm.

c. The customers are sorted once more, this time in ascending order of the overall priorities ε_i^{η}, and a ranking weight $(v_u - k)$ (denoted by ω_i^{η}) is assigned to customer i ranked at the k^{th}position of the list. This last sorted list is called the *Candidate List*. For each customer in the *Candidate List*, we calculate a cost value by dividing the number of unrouted customers (v_u), with the ranking weight ω_i^{η} of the specific customer in the Candidate List (equation (37)). The emerging cost value S_i^{η} of customer i is normalized (equation (38)) by dividing it with the average of the past cost values of customer i calculated in the previous $\eta - 1$ iterations (denoted by A_i^{η}).

The resulting normalized value is denoted by φ_i^η and $A_i^\eta = \frac{\sum_{i=1}^{\eta-1} \varphi_i^\eta}{(\eta-1)}$. Finally, based on the normalized values φ_i^η we calculate the probability ε_i^η of selecting customer i by formula (39) (Ríos-Mercado & Fernández, 2009).

$$S_i^\eta = \frac{\nu_u}{\omega_i^\eta} \tag{37}$$

$$\varphi_i^\eta = \frac{S_i^\eta}{A_i^\eta} \tag{38}$$

$$\varepsilon_i^\eta = \frac{f_i^\eta}{\sum_{h=1}^{n_u} f_h^\eta} \tag{39}$$

where:

- S_i^η: Cost value of customer i in iteration η
- ν_u: Number of customers remaining to be inserted in a route
- z_i^η: Rank of customer i in Candidate List (in iteration η)
- φ_i^η: Frequency of customer i
- A_i^η: Average cost value for customer i, resulting from all the previous $(\eta - 1)$ iterations
- ε_i^η: Probability of selection for customer i in iteration η

ii. The selected customer in step (i) is assigned to the first available truck with the greatest volume capacity that the order fits in. If no truck has enough remaining capacity for the specific customer, a new route is initiated. In any case, the selected customer is inserted in the position of the route that induces the minimum increase of the average transportation risk. It is worth noticing that the risk calculation during the route construction process assumes average travel speeds on the links. This assumption is essential since at this phase the loading start time of the trucks and the corresponding departure time of the routes have not been determined yet.

iii. After the insertion of the selected customer, it is removed from the ranking lists and the Candidate List, and the process returns to step (i). The process terminates when all the customers have been assigned to a truck.

The output of this insertion procedure is a list of routes assigned to a list of delivery trucks servicing all the orders. The emerging solution is enhanced with a feasible schedule of the corresponding loading activities, i.e., the assignment of each route to a loading station for a certain number of subsequent slots. It is worth noticing that the start time of each loading activity is determined so that the corresponding route risk is minimized. The scheduling process is provided in Appendix D.

4. Experiments and Results

4.1 Experimental Data

The proposed algorithm was coded in Java. The experiments were performed on a computer with a 3.60GHz Intel® Core™ i7-4790 CPU and a 16 GB RAM. The purpose of our experiments is to assess: i) the effectiveness of the novel components of the proposed algorithm (i.e., the new One-Point Crossover operator and the new Multi-point Crossover operator) in determining the efficient frontier of the problem, and ii) the efficiency of the two feasibility methods in resolving any capacity violation issues. Three alternative configurations of the proposed algorithm were tested:

- *Configuration 1 (Conf-1)*: The NSGA-II was tuned to use solely the Multi-point Crossover operator for reproduction and the Route Splitting method for resolving any capacity violation issues.
- *Configuration 2 (Conf-2)*: The NSGA-II was tuned to use the conventional reproduction operators (one-point crossover and the mutation supported by binary tournament, where the use of each operator is randomly selected for each NSGA-II iteration) and the Relocation method for resolving any capacity violation issues.
- *Configuration 3 (Conf-3)*: The NSGA-II was tuned to use the conventional reproduction operators (one-point crossover and mutation supported by binary tournament) and the Route Splitting method for resolving any capacity violation issues.

The experiments were carried out on the benchmark instances GT_13-20 introduced by Golden et al. (1984), customized accordingly to fit the proposed problem. Each of the test problems was solved by the proposed algorithm under the configurations 1-3. The specific instances contain 50, 75, or 100 customers and a fleet of 7 to 14 vehicles grouped into 6 different types (Cruz et al., 2014). For the purpose of the experiments, a base travel speed of 40 km/h is assumed, which is adjusted dynamically by 0% to 50% depending on the time of day. Additionally, the links between customers are assumed to have an average population density ranging from 1,000 to 15,500 people per square kilometer. Moreover, Table 2 presents the value of the impact radius as a function of the load of the truck (in liters).

The experiments aimed at the comparative assessment of: i) the performance of the New Multi-Point Crossover Operator over the performance of the One-point Crossover operator and mutation supported by binary tournament by comparing the results of Conf-1 vs. the results of Conf-3, and ii) the performance of the two different methods for attaining feasibility (Relocation Method vs Splitting method) by comparing the results of Conf-2 vs. the results of Conf-3.

Transported Quantity (lt)	Impact Radius (m)
0	0
(0-5,000]	40
(5,000-10,000]	60
(10,000-15,000]	80
(15,000-20,000]	100
>20,000	120

Table 2: Assumed impact radius according to the transported volume quantity.

The metrics used for the evaluation of the algorithm's results are presented below. The Spacing metric and the Hypervolume indicator have been widely utilized in the evaluation of results for various Bi-objective Vehicle Routing Problems. For example, in Baños et al. (2013) both metrics have been used for the result evaluation of an NSGA-II algorithm used over a multi-objective vehicle routing problem.

1. The *spacing metric* measures the distribution of solutions in a solution set, where a larger value indicates a more spread-out or diverse set of solutions, reflecting greater variation among them. The formulation and the detailed analysis of the metric is provided in Appendix E.
2. *Hypervolume indicator* measures the quality of a set of solutions based on their coverage of the objective space. A higher hypervolume value indicates that the non-dominated solutions determined are diverse and well-distributed across the objective space. The formula and further details are provided in Appendix E.
3. *Risk Values Range* expressed by the minimum and maximum risk values (min risk, max risk) over the set of solutions. The risk is expressed in person hours.
4. *Distance Values Range* expressed by the minimum and maximum traveled distance (min distance, max distance) over the set of solutions. The data sets used for the experiments utilize fabricated coordinates that do not correspond directly to any specific units of measurement. Consequently, we can say that our distance results are expressed in travel units.
5. *Computational Time* (seconds) required for the execution of the proposed algorithm.

Each of the experimental runs involved the generation of an initial population of 50 solutions through the GRASP method followed by 500 iterations of the NSGA-II algorithm.

4.2 Tuning the Multi-Point Crossover Operator

The Multi-Point Crossover Operator is a crucial component of the proposed algorithm which employs a reproduction process consisting of four distinct steps. Each step selectively introduces a predetermined percentage of customers from the parental solutions into the offspring population. In Figure 7, we present the hypervolume % results obtained by examining different percentage scenarios (Conf-1 for GT_20). The four scenarios of percentages are outlined as follows in Table 3:

Combination	**Step 1**	**Step 2**	**Step 3**	**Step 4**
Selection-1	40%	30%	10%	20%
Selection-2	20%	10%	30%	40%
Selection-3	20%	20%	20%	40%
Selection-4	20%	30%	30%	20%

Table 3: Percentage combinations for each step of the Multi-Point Crossover used for the percentage exploration.

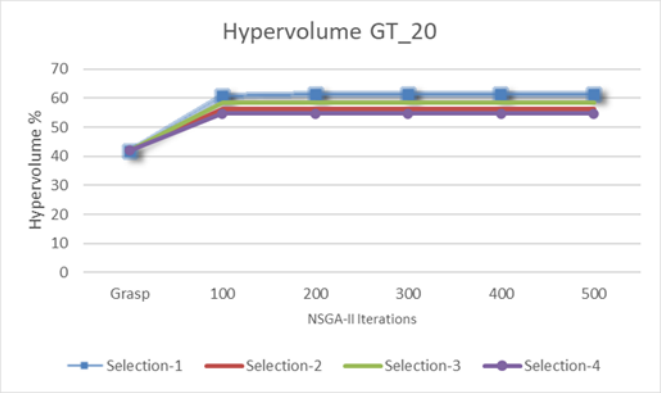

Fig. 7: Hypervolume% comparison for different percentage combinations utilized in the Multi-Point Crossover Operator (Conf-1 for GT_20).

Our analysis of the results presented in Figure 7 reveals that the percentage scenario Selection-1 consistently yields marginally superior outcomes in terms of the Hypervolume % metric. As a result, we have selected to employ the Selection-1 scenario for all the tests presented above which utilize the Multi-Point Crossover Operator.

4.3 Assessing the Operators' Performance

Graphs 1-8 illustrated in Figure 8, present the hypervolume indicator of the population of solutions determined at various stages of the proposed algorithm for problem instances GT_13 to GT_20 respectively. Each graph shows the hypervolume indicator evolution with a step of 100 iterations starting with the initial population of solutions until 500 iterations are completed. The graphs indicate the results for each of the three configurations separately, using a different color and shape (blue & square for Conf-1, red & triangle for Conf-2, and green & circle for Conf-3).

Upon careful examination of graphs 1-8, the following remarks can be made:

- The performance of the algorithm under Conf-1 (with the Multi-point Crossover operator) is similar to or higher than the performance of the algorithm under Configuration 3 (with the conventional reproduction operators i.e. one-point crossover and mutation supported by binary tournament). In more detail, it can be observed that the performance of Conf-1 (blue line with squares) is similar to the performance of Conf-3 (green line & circles) in 4 out of the 8 graphs and superior in 3 out of the 8 graphs. This observation indicates that the new Multi-Point Crossover operator (used in Conf-1) yields solutions that exhibit closer proximity to the Pareto Front than the solutions determined by the one-point crossover & mutation supported by binary tournament operators (used in Conf-3).
- The hypervolume indicator of the solutions determined by the proposed algorithm under Conf-2 (one-point crossover & mutation supported by binary tournament enhanced with the Relocation method) surpasses the corresponding hypervolume indicator of the solutions determined under Conf-3 (one-point crossover & mutation supported by binary tournament enhanced with the Route Splitting method) in 7 out of out the 8 instances. This observation suggests that fixing capacity violation issues with the Relocation Method (used

in Conf-2) has the potential to enhance the algorithm's performance more than the corresponding implementation with the Route Splitting Method (used as in Conf-3).

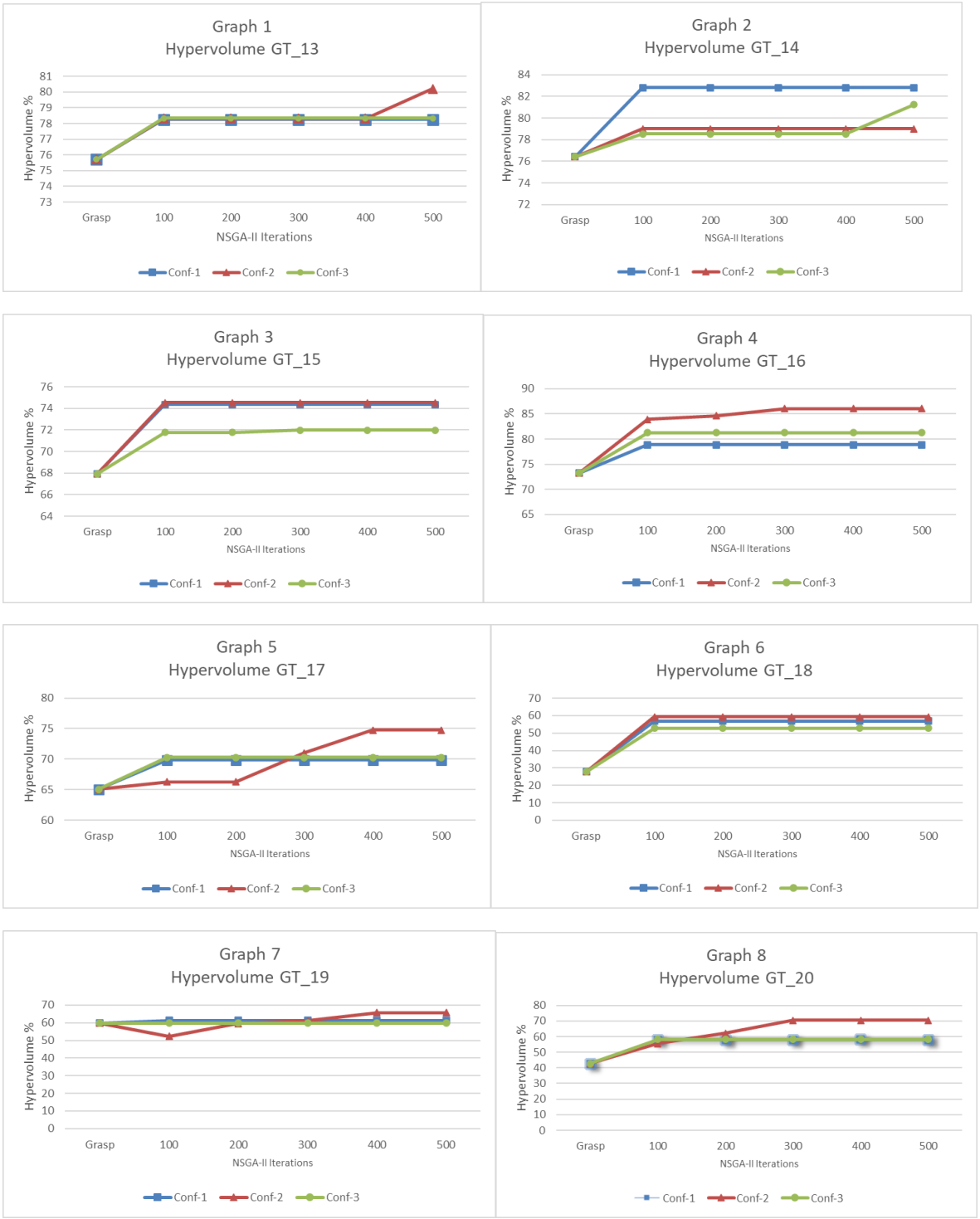

Fig. 8: Graphs 1-8 presenting the Hypervolume indicator of Conf. 1, 2 & 3 for the instances GT_13 to GT_20.

Table 4 presents the percentage increase of the hypervolume indicator throughout the execution of the 500 iterations of NSGA-II using the hypervolume indicator achieved by Grasp as a reference value. The data presented in the table indicates that the most significant

enhancement in the hypervolume outcomes occurs during the first 100 iterations. Each dataset features a fixed fleet of vehicles, with capacities closely aligned with the total ordered volume. As a result, there is limited room for improvement due to the constrained capacity, presenting a challenging environment for optimization. Moreover, we notice that in most of the cases, the initial solutions of Grasp provide a relatively high Hypervolume value. Consequently, as in some cases NSGA-II tries to avoid being trapped in local optimum, we have observed that the NSGA-II algorithm can provide worse results in its first iterations vs the Reactive Grasp algorithm, before resulting in improved solutions (GT_19 in Conf-2).

DATASET	**Type of Test**	**Multi-Point Crossover**	**SPLIT**	**100 ITER**	**200 ITER**	**300 ITER**	**400 ITER**	**500 ITER**
	Conf-1	YES	YES	3%	3%	3%	3%	3%
GT_13	Conf-2	NO	NO	3%	3%	3%	3%	6%
	Conf-3	NO	YES	3%	3%	3%	3%	3%
	Conf-1	YES	YES	8%	8%	8%	8%	8%
GT_14	Conf-2	NO	NO	3%	3%	3%	3%	3%
	Conf-3	NO	YES	3%	3%	3%	3%	6%
	Conf-1	YES	YES	9%	9%	9%	9%	9%
GT_15	Conf-2	NO	NO	10%	10%	10%	10%	10%
	Conf-3	NO	YES	6%	6%	6%	6%	6%
	Conf-1	YES	YES	8%	8%	8%	8%	8%
GT_16	Conf-2	NO	NO	15%	16%	17%	17%	17%
	Conf-3	NO	YES	11%	11%	11%	11%	11%
	Conf-1	YES	YES	7%	7%	7%	7%	7%
GT_17	Conf-2	NO	NO	2%	2%	9%	15%	15%
	Conf-3	NO	YES	8%	8%	8%	8%	8%
	Conf-1	YES	YES	105%	105%	105%	105%	105%
GT_18	Conf-2	NO	NO	113%	113%	113%	113%	113%
	Conf-3	NO	YES	90%	90%	90%	90%	90%
	Conf-1	YES	YES	2%	2%	2%	2%	2%
GT_19	Conf-2	NO	NO	-13%	0%	2%	10%	10%
	Conf-3	NO	YES	0%	0%	0%	0%	0%
	Conf-1	YES	YES	36%	36%	36%	36%	36%
GT_20	Conf-2	NO	NO	30%	46%	65%	65%	65%
	Conf-3	NO	YES	37%	37%	37%	37%	37%

Table 4: Percentage improvement of the Hypervolume indicator during the 500 iterations of NSGA-II compared with the Grasp output.

Figure 9 illustrates graphs 9 to 16 that present the spacing metric performance of the proposed algorithm in problem instances GT_13 to GT_20, respectively. No definite indication can be deduced from these graphs. It can be noticed that the spacing metric of the solutions determined by the proposed algorithm under Conf-1 (using the New Multi-point Crossover Operator) surpasses the corresponding metric of the solutions determined by Conf-3 (using the one-point crossover & mutation supported by binary tournament) in 5 out of the 8 graphs. Moreover, Graphs 9-16 indicate that the spacing metric of the solution determined by Conf-2 (using the Relocation Method for fixing capacity violations) surpasses the corresponding metric of the solutions determined by Conf-3 (using the Route Splitting method) in 6 out of the 8 graphs.

Fig. 9: Graphs 9-16 presenting the Spacing metric of Conf. 1, 2 & 3 for the instances GT_13 to GT_20

Table 5 presents the average value of the assessment metrics Hypervolume % and Spacing across all 500 iterations. In addition, the table also presents the min Risk and min Distance retrieved over all NSGA-II iterations (500 in total) executed for Conf. 1-3. From Table 5 we can observe that:

- The avg hypervolume % of Conf-1 (using the Multi-Point Crossover Operator) outperforms in all instances the corresponding results of Conf- 3 (using the one-point crossover and mutation supported by binary tournament). The same observation was also made from

graphs 1 to 8 (Fig. 8) which suggests that the Multi-Point Crossover Operator outperforms the conventional reproduction operators.

- The avg hypervolume % of Conf-2 that uses the Relocation method for generating feasible solutions outperforms in most instances the results of Conf-3 that uses the Splitting method for the same purpose (both using the one-point crossover and mutation supported by binary tournament for the solution generation). Similar results have also been driven by the graphs 1 to 8 (Fig. 8).
- The average spacing of Conf-2 outperforms in most instances the results of Conf-3. The same observation was also made from graphs 9 to 16 (Fig. 9).

DATASET	Cust #	Type of Test	Multi-Point Crossover	SPLIT	Avg Hypervol.%	Avg Spacing	Min Risk	Min Dist
GT_13	50	Conf-1	YES	YES	76,6%	2536	553	1578
		Conf-2	NO	NO	76,6%	2603	527	959
		Conf-3	NO	YES	72,3%	3424	503	837
GT_14	50	Conf-1	YES	YES	76,3%	2992	515	1492
		Conf-2	NO	NO	68,3%	7991	503	870
		Conf-3	NO	YES	72,0%	3809	501	1046
GT_15	50	Conf-1	YES	YES	67,5%	3779	529	1662
		Conf-2	NO	NO	66,9%	4806	512	711
		Conf-3	NO	YES	65,7%	3208	511	824
GT_16	50	Conf-1	YES	YES	73,4%	4706	514	1592
		Conf-2	NO	NO	71,7%	2584	501	963
		Conf-3	NO	YES	69,8%	3501	515	835
GT_17	75	Conf-1	YES	YES	68,4%	6423	602	2195
		Conf-2	NO	NO	60,3%	6817	509	1500
		Conf-3	NO	YES	52,4%	10723	519	1323
GT_18	75	Conf-1	YES	YES	55,1%	9957	505	2265
		Conf-2	NO	NO	43,5%	22144	509	1409
		Conf-3	NO	YES	50,2%	13165	509	1007
GT_19	100	Conf-1	YES	YES	54,3%	2818	2394	3241
		Conf-2	NO	NO	47,5%	8392	670	2117
		Conf-3	NO	YES	47,9%	4040	510	1829
GT_20	100	Conf-1	YES	YES	45,4%	4369	567	2997
		Conf-2	NO	NO	50,3%	5218	855	1735
		Conf-3	NO	YES	44,7%	5766	512	1759

Table 5: Results for the Datasets GT_13 to GT_20 when performing Conf. 1, 2 & 3.

Based on the reported data, it can be deduced that the adoption of the New Multi-Point Crossover Operator and the Customer Relocation method, may yield more advantageous outcomes in comparison to employing the original operators of NSGA-II alongside the straightforward Route Splitting method. Moreover, the utilization of the suggested model formulation enables us to mimic real-world scenarios and provide an optimized routing solution that takes into account the HazMat risk.

4.4 Computational Time Performance

Table 6 provides the computational time required for each of the two phases of the proposed algorithm: i) the execution of the Grasp algorithm, and ii) the execution of 500 iterations of the NSGA-II. It becomes evident that the computational time of the Grasp algorithm is exceedingly minimal. Moreover, it is worth noting that the use of the Multi-Point Crossover Operator requires double the computational time compared with the one-point crossover & mutation supported by binary tournament operators. It also can be observed that increasing the population or expanding the fleet size for a given population leads to a corresponding increase in computational time mainly when the Multi-Point Crossover Operator is used (Conf.1) e.g. from GT_18 with 75 customers to GT_19 with 100 customers.

DATASET	Cust #	Veh. #	Type of Test	Multi-Point Crossover	SPLIT	Comp. Time GRASP (sec)	Comp. Time NSGA-II (sec)
GT_13	50	17	Conf-1	YES	YES	2	117
			Conf-2	NO	YES	1	70
			Conf-3	NO	NO	1	68
GT_14	50	7	Conf-1	YES	YES	2	118
			Conf-2	NO	YES	2	54
			Conf-3	NO	NO	1	51
GT_15	50	9	Conf-1	YES	YES	1	121
			Conf-2	NO	YES	1	57
			Conf-3	NO	NO	1	61
GT_16	50	9	Conf-1	YES	YES	2	114
			Conf-2	NO	YES	2	58
			Conf-3	NO	NO	1	59
GT_17	75	11	Conf-1	YES	YES	2	144
			Conf-2	NO	YES	2	75
			Conf-3	NO	NO	2	75
GT_18	75	14	Conf-1	YES	YES	2	153
			Conf-2	NO	YES	3	75
			Conf-3	NO	NO	2	76
GT_19	100	10	Conf-1	YES	YES	4	185
			Conf-2	NO	YES	4	71
			Conf-3	NO	NO	5	73
GT_20	100	13	Conf-1	YES	YES	3	188
			Conf-2	NO	YES	4	91
			Conf-3	NO	NO	2	87

Table 6: Computational time of Grasp and NSGA-II method for Conf-1, 2 & 3 for the instances GT_13 to GT_20.

5. Conclusion

This paper focuses on the vehicle routing problem in urban areas for the transportation of Hazardous Materials. The research presents a novel element, in particular the scheduling of the loading operations at the available loading station, which enriches the current framework. A bi-objective formulation has been developed with the first objective being the total traveled distance whereas the second objective is risk minimization. With our model formulation, we have tried to approach real-life scenarios by taking into consideration the start time of each

vehicle's route which is respectively correlated with the actual travel time and the risk. In our risk assessments, we have also taken into account the actual load being transported by each truck at every point along its route. The genetic algorithm NSGA-II was employed to address the model, as it is a highly effective approach for addressing bi-objective vehicle routing problems. In our formulation, we have incorporated supplementary techniques that encompass all aspects of our model. One of the methods implemented is the New Multi-Point Crossover operator, which seeks to enhance the level of diversity within the solution space. The evaluation of our formulation's outcomes has been conducted using the Hypervolume and Spacing metrics. The analysis demonstrates that the inclusion of the New Multi-Point Crossover operator in the NSGA-II formulation yields a more diverse set of solutions and achieves a better tradeoff between the two objectives. Nevertheless, after including the risk factors in our model, it becomes evident that there is an increase in the overall traveled distance.

In conclusion, the inclusion of load and time dependency in our model enhances the accuracy of risk calculations, allowing for a more realistic representation of real-life scenarios. This, in turn, facilitates a more precise evaluation of potential risks and enables effective risk mitigation strategies.

Declaration of competing interest

The authors declare that they have no known competing financial interests or personal relationships that could have appeared to influence the work reported in this paper.

Acknowledgments

This research is co-financed by Greece and the European Union (European Social Fund- ESF) through the Operational Programme «Human Resources Development, Education and Lifelong Learning» in the context of the project "Strengthening Human Resources Research Potential via Doctorate Research – 2nd Cycle" (MIS-5000432), implemented by the State Scholarships Foundation (IKY).

Appendix A: The trade-off between Distance and HazMat Risk

The Mixed Integer Linear Programming (MILP) formulation presented in section 2.3 is solved to optimality through the implementation of the ε-constraint method. This approach allows us to address the bi-objective nature of the problem by prioritizing one objective while constraining the other. Specifically, the ε-constraint formulation is implemented through the CPLEX API in Java, where risk is kept as the objective function, and distance is constrained by the parameter ε. This methodology highlights the trade-offs between the two objectives and provides a set of solutions from which a decision-maker can choose, balancing cost (distance) and risk.

To illustrate this, a problem instance involving two trucks with capacities of 21,000 liters and 15,000 liters, respectively, and six customers are considered. The average population density per square kilometer along the routes between customers and the depot varies significantly, ranging from 1,600 to 12,000 individuals per square kilometer. Additionally, the travel speed across these links is influenced by the time of day the trucks traverse each segment, resulting in travel times that range between 5 and 55 minutes. The order volumes for each customer are displayed in Table 1a.

The risk measure, in this case, expresses the time duration during which the potentially affected population remains in danger. Thus, the trade-off in routing trucks is expressed as the additional population time exposure incurred per kilometer reduction in travel distance. By analyzing these results, we gain valuable insights into how the prioritization of one objective impacts the outcomes related to the other, aiding decision-makers in selecting the most appropriate solution based on their preferences.

Customer	Order vol (lt)
1	5,000
2	3,000
3	6,000
4	7,000
5	9,000
6	2,000

Table 1a: Order volume in liters per customer

The table below (table 2a) demonstrates the results of Risk and Distance for all the trade-off points when distance is constrained. A notable observation is that, as the distance decreases, reflecting more efficient routing, the associated risk increases significantly. For example, reducing the distance from 198 to 88 units (a 55% decrease) leads to a rise in risk from 7,127 to 15,217 (a 113% increase). The relationship is non-linear, as seen between points 1 and 2, where a substantial distance reduction occurs with only a slight increase in risk, while between points 5 and 6, the risk escalates significantly for a more modest distance gain. These results emphasize the complexity of balancing efficiency and safety, showing that minimizing distance may lead to considerable compromises in safety, while prioritizing lower risk may result in longer travel routes. This analysis underscores the importance of weighing priorities carefully

based on the specific requirements of the decision-making context. The trade-off described above is also demonstrated in Fig. 1a.

Trade-off points	Risk	Distance
1	7127	198
2	7178	156
3	8803	153
4	9723	137
5	12345	122
6	15217	88

Table 2a: Results of Risk and Distance for all the Trade-off points.

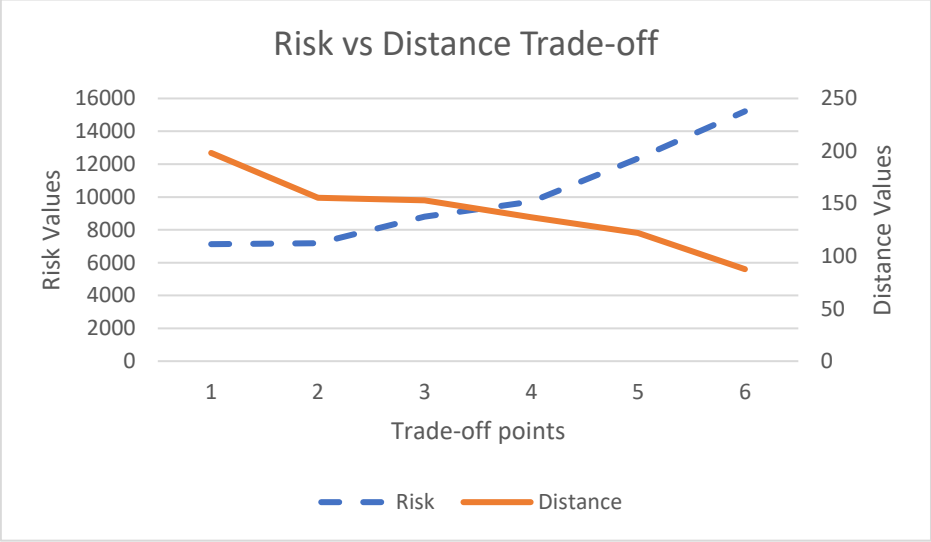

Fig. 1a: Trade-off between Risk and Distance.

Appendix B: NSGA-II Algorithm Pseudocode

```
NSGA-II MAIN LOOP
Function NSGA_II
INPUT: parent_pop // of size N
WHILE child_pop <N
   FOR i=0 to parent_pop
    PERFORM: randomly crossover OR binary tournament & mutation to parent_pop
     CREATE child
     child_pop++
     END FOR
  END WHILE
pop= parent_pop+ child_pop

FOR i=0 to pop.size
  CALCULATE: risk[i], dist[i]
END FOR
PERFORM: Non Dominated Sort of pop
WHILE final_pop.size<N
  FOR j=0 to set.size //population sets after non-dominated rank
      IF set[j].size+ final_pop.size <N
         final_pop.add(set[j])
       ELSE
          Calculate: Crowding distance of set[j]
            UNTIL final_pop.size ==N
                     SELECT item of set[j] with biggest crowding distance AND
                              final_pop.add(pop.set[j].item[k])
             END
          END IF
    END FOR
END WHILE
```

Appendix C: Pseudocode for Customer Relocation Method

```
INPUT: route, veh, distances

FOR v = 0 to veh_no
      Calculate:  loaded quantity in vehicle v

   Select: the vehicle v to be assessed for feasibility

   FOR each customer c in c_route
      IF loaded_qty[v]+ customer_qty[c]<max_weight[v] //the order volume can fit in the current vehicle
         Assign: customer c to vehicle v
        loaded_qty[v]= loaded_qty[v]+ customer_qty[c] //Update the remaining volume assigned vol. of vehicle
      ELSE
         limit_exceeded =true
        z=0
        WHILE limit_exceeded =true
            //search if the order can fit in other vehicles
           IF loaded_qty[z]+ customer_qty[c]<max_weight[z]
                Assign: customer c to vehicle z
                loaded_qty[z]= loaded_qty[z]+ customer_qty[c]
                limit_exceeded=false
          ELSE
               z++
          END IF

           IF   z==total_vehs -1 AND limit_exceeded==true
             Remove: from route ½assigned customers
            Start the assessment process from the beginning
         END IF

       END WHILE
      END IF

    FOR v = 0
      //re-arrange the route to give the best customer sequence by considering risk and distance
      CALL Re-assignment method (new_route, veh V)
    END FOR

  RETURN new_route
```

Appendix D: Pseudocode for Scheduling the Loading Activities

FOR v=0 to total_vehicles
Compute: assigned order volume q[v] per vehicle v
Compute: required service time t[v] of vehicle v at a pump p according to q[v]
Compute: required number of slots s at loading station p according to t[v]
END FOR
FOR p=0 to loading stations
Assign: available start time of service per loading station s_e $=$ *open time of depot*
END FOR

WHILE there are vehicles v that have been assigned with orders and remain unassigned to a loading station

Select: earliest available loading station p
FOR v=0 to total_vehicles
Calculate: Risk of vehicle v if assigned to loading station p
END FOR
Get: v that results in minimum risk
Assign: v to selected loading station p
Set: the new available start time of loading station $s_e = s * x + s_t$ *// x is an integer number*

END WHILE

RETURN Loading Stations Schedule

Appendix E: Analysis and Definition of Performance Metrics

Spacing Metric

The spacing metric is used to measure the distribution or spread of solutions in a multi-objective optimization problem. It assesses how well the solutions are spaced across the objective space, with the goal of ensuring diversity in the set of solutions. The metric takes into account the pairwise distances between solutions, aiming to evaluate how dispersed the solutions are without considering their exact values in terms of the objectives.

The formula for the calculation of the spacing metric is:

$$Spacing = \frac{1}{n_0(n_0-1)} \sum_{\kappa=1}^{n_0} \sum_{\mu=1,\mu\neq\kappa}^{n_0} d(P_\kappa, P_\mu)$$

where:

- P_κ, P_μ: represent the $\kappa^{\text{th}}$and μ^{th}solutions in the set
- $d(P_\kappa, P_\mu)$: denotes the Euclidian distance between solutions P_κ and P_μ in the objectives space (defined by distance and risk)
- n_0: number of solutions

Hypervolume indicator

The hypervolume indicator is a performance metric used to evaluate the quality of a Pareto front in multi-objective optimization problems. It provides a quantitative measure of the volume of the objective space that is dominated by the Pareto front, bounded by a predefined reference point. A higher hypervolume value indicates a better approximation of the true Pareto front, as it covers a larger portion of the objective space.

The calculation of the hypervolume indicator begins by defining a reference point in the objective space. This reference point is typically selected based on the worst values for each objective function, such as the maximum value of each objective in the obtained set of solutions. Once the reference point is established, the hypervolume is calculated as the volume of the objective space that lies between the Pareto front and the reference point.

Calculation Formula

The hypervolume percentage is given by:

$$Hypervolume\ \% = \frac{\sum_{\kappa=0}^{no} HIncrement_\kappa}{Total\ volume} \cdot 100$$

where:

- no: number of solutions
- μ: number of objectives
- $\sum_{\kappa=0}^{n_0} HIncrement_\kappa$ =The incremental volume contributed by the κ-th solution to the overall hypervolume.

Incremental Hypervolume Calculation
The incremental hypervolume contribution from each solution is calculated as follows:

$$\sum_{\kappa=0}^{n_0} HIncrement_\kappa = currentVol_\kappa - previousVol$$

where:

- $currentVol_\kappa$ =The hypervolume of the objective space dominated by the solution κ.
- $previousVol_i =$ The hypervolume contributed by the previous solution $\kappa - 1$.

$currentVol_\kappa$ is calculated using:

$$currentVol_\kappa = \Pi_{j=1}^{\mu} \max(0, upperBound_j - ObjValue_{ij})$$

where:

- $upperBound_j$: The upper bound value for objective j as defined by the reference point.
- $ObjValue_{ij}$; The objective value for solution κ concerning objective j.

References

Androutsopoulos, K & Zografos G, K. (2010). Solving the bicriterion routing and scheduling problem for hazardous materials distribution. Transportation Research Part C, 18(5), 713-716. doi: 10.1016/j.trc.2009.12.002

Araee, E., Manavizadeh, N., & Aghamohammadi Bosjin, S. (2020). Designing a multi-objective model for a hazardous waste routing problem considering flexibility of routes and social effects. Journal of Industrial and Production Engineering, 37(1), 33-45. doi: 10.1080/21681015.2020.1727970

Baños, R., Ortega, J., Gil, C., Márquez, A. L., & De Toro, F. (2013). A hybrid meta-heuristic for multi-objective vehicle routing problems with time windows. Computers & Industrial Engineering, 65(2), 286-296. doi: 10.1016/j.cie.2013.01.007

Batta, R., & Chiu, S. S. (1988). Optimal Obnoxious Paths on a Network: Transportation of Hazardous Materials. Operations Research, 36(1), 84–92. doi:10.1287/opre.36.1.84

Bronfman, A., Marianov, V., Belmar, G., P., Villagra, A., L. (2015). The maximin HAZMAT routing problem. European Journal of Operational Research, 241, 15–27. doi: 10.1016/j.ejor.2014.08.005

Bula, G. A., Afsar, H. M., González, F. A., Prodhon, C., & Velasco, N. (2019). Bi-objective vehicle routing problem for hazardous materials transportation. Journal of Cleaner Production, 206, 976-986. doi: 10.1016/j.jclepro.2018.09.228

Carotenuto, P., Giordani, S., & Ricciardelli, S. (2007). Finding minimum and equitable risk routes for hazmat shipments. Computers & Operations Research, 34(5), 1304–1327. doi:10.1016/j.cor.2005.06.003

Chai, H., He, R., Kang, R., Jia, X., & Dai, C. (2023). Solving Bi-Objective Vehicle Routing Problems with Driving Risk Consideration for Hazardous Materials Transportation. Sustainability, 15(9), 7619. doi: 10.3390/su15097619

Cruz, C., J., Grasas, A., Ramalhinho, H., Angel, J., A. (2014). A savings-based randomized heuristic for the heterogeneous fixed fleet vehicle routing problem with multi-trips. Journal of Applied Operational Research, 6(2), 69-81

Deb, K., Agarwal, S., Pratap, A., & Meyarivan, T. (2000). A Fast Elitist Non-dominated Sorting Genetic Algorithm for Multi-objective Optimization: NSGA-II. In: Schoenauer, M., et al. Parallel Problem Solving from Nature PPSN VI. PPSN 2000. Lecture Notes in Computer Science, vol 1917. Springer, Berlin, Heidelberg. doi:10.1007/3-540-45356-3_83

Deb, K., Pratap, A., Agarwal, S., & Meyarivan, T. (2002). A fast and elitist multiobjective genetic algorithm: NSGA-II. IEEE Transactions on Evolutionary Computation, 6(2), 182–197. doi:10.1109/4235.996017

DOT U.S. (2022). 10 Year Incident Summary Reports. https://portal.phmsa.dot.gov/analytics/saw.dll?Portalpages Large

DOT U.S., (2017). Hazardous Materials Shipments by Transportation Mode. https://www.bts.gov/browse-statistical-products-and-data/freight-facts-and-figures/hazardous-materials-shipments

Erkut, E., & Alp, O. (2007). Integrated Routing and Scheduling of Hazmat Trucks with Stops En Route. Transportation Science, 41(1), 107–122. doi:10.1287/trsc.1060.0176

Erkut, E., & Glickman, T. (1997). Minimax Population Exposure in Routing Highway Shipments of Hazardous Materials. Transportation Research Record: Journal of the Transportation Research Board, 1602, 93–100. doi:10.3141/1602-14

Erkut, E. and V. Verter (1998). Modeling of Transport Risk for Hazardous Materials. Operations Research, Vol. 46, No. 5, pp. 625-642.

Frank, W., C., Thill, J., C., Batta, R. (2000). Spatial decision support system for hazardous material truck routing. Transportation Research Part C, 8, 337-359. doi: 10.1016/S0968-090X(00)00007-3

Golden, B., Assad, A., Levy, L., Gheysens, F. (1984). The fleet size and mix vehicle routing problem. Computers and Operations Research, 11(1), 49-66. doi: 10.1016/0305-0548(84)90007-8

Jaikishan, T. S. & Patil, R. (2019). A Reactive GRASP Heuristic Algorithm for Vehicle Routing Problem with Release Date and Due Date Incurring Inventory Holding Cost and Tardiness Cost. IEEE International Conference on Industrial Engineering and Engineering Management (IEEM), 1393-1397, doi:10.1109/IEEM44572.2019.8978851.

Marinakis, Y., Migdalas, A., & Pardalos, P. M. (2007). A new bi-level formulation for the vehicle routing problem and a solution method using a genetic algorithm. Journal of Global Optimization, 38(4), 555–580. doi:10.1007/s10898-006-9094-0

Men, J., Jiang, P., Xu, H., Zheng, S., Kong, Y., Hou, P., & Wu, F. (2020). Robust multi-objective vehicle routing problem with time windows for hazardous materials transportation. IET Intelligent Transport Systems, 14(3), 154-163. doi: 10.1049/iet-its.2019.0332

Moura, A., & Oliveira, J. F. (2009). An integrated approach to the vehicle routing and container loading problems. OR Spectrum, 31(4), 775–800. doi:10.1007/s00291-008-0129-4

Panicker, V. V., & Mohammed, I. O. (2018). Solving a heterogeneous fleet vehicle routing model-A practical approach. 2018 ieee international conference on system, computation, automation and networking (icscan), 1-5. doi: 10.1109/ICSCAN.2018.8541149

Pradhananga, R., Taniguchi, E., Yamada, T., Qureshi, A., G. (2014). Bi-objective decision support system for routing and scheduling of hazardous materials. Socio-Economic Planning Sciences, 48(2), 135-148. doi: 10.1016/j.seps.2014.02.003

Ríos-Mercado, R. Z., & Fernández, E. (2009). A reactive GRASP for a commercial territory design problem with multiple balancing requirements. Computers & Operations Research, 36(3), 755-776.

Shifeng Niu, Satish V. Ukkusuri (2020). Risk Assessment of Commercial dangerous - goods truck drivers using geo-location data: A case study in China. Accident Analysis & Prevention, 137, 105427. doi:10.1016/j.aap.2019.105427

Wang, N., Zhang, M., Che, A., & Jiang, B. (2017). Bi-objective vehicle routing for hazardous materials transportation with no vehicles travelling in echelon. IEEE Transactions on Intelligent Transportation Systems, 19(6), 1867-1879. doi: 10.1109/TITS.2017.2742600

Wang, X., Tang, X., Fan, T., Zhou, Y., & Yang, X. (2024). Commercial Truck Risk Assessment and Factor Analysis Based on Vehicle Trajectory and In-Vehicle Monitoring Data. Transportation Research Record, 2678(12), 1428-1443. doi:10.1177/03611981241252148

Zero, L., Bersani, C., Paolucci, M., & Sacile, R. (2019). Two new approaches for the bi-objective shortest path with a fuzzy objective applied to HAZMAT transportation. Journal of Hazardous Materials, 375, 96–106. doi:10.1016/j.jhazmat.2019.02.101

Zhang, M., Wang, N., He, Z., Yang, Z., & Guan, Y. (2018). Bi-Objective Vehicle Routing for Hazardous Materials Transportation With Actual Load Dependent Risks and Considering the Risk of Each Vehicle. IEEE Transactions on Engineering Management, 1–14. doi:10.1109/tem.2018.2832049

Zhang, J., Wang, G., Sheng, Q., Jia, X., & Xie, P. (2023). Multi-Depot Heterogeneous Vehicle Routing Optimization for Hazardous Materials Transportation. IEEE Access. doi: 10.1109/ACCESS.2023.3300041

Zhao, J., & Zhu, F. (2016). A multi-depot vehicle-routing model for the explosive waste recycling. International Journal of Production Research, 54(2), 550-563. doi: 10.1080/00207543.2015.1111533

Zografos, K. G., & Androutsopoulos, K. N. (2004). A heuristic algorithm for solving hazardous materials distribution problems. European Journal of Operational Research, 152(2), 507–519. doi:10.1016/s0377-2217(03)00041-9

Zografos, K. G., & Davis, C. F. (1989). Multi-Objective Programming Approach for Routing Hazardous Materials. Journal of Transportation Engineering, 115(6), 661–673. doi:10.1061/(asce)0733-947x(1989)115:6(661)